

UCSD/PTH/97-33
OHSTPY-HEP-T-97-016
hep-lat/9712016

One-loop matching of lattice and continuum heavy-light axial vector currents using NRQCD

Colin J. Morningstar

Dept. of Physics, University of California at San Diego, La Jolla, California 92093-0319

J. Shigemitsu

Physics Department, The Ohio State University, Columbus, OH 43210

(December 15, 1997)

Abstract

The temporal component of the heavy-light axial vector current is constructed to one-loop order in perturbation theory and to order $1/M$, where M is the heavy quark mass, in terms of operators suitable for use in lattice simulations of B and D mesons. The $O(a)$ -improved clover action is used for the massless light quark, where a is the lattice spacing, and propagation of the heavy quark is described by a nonrelativistic lattice action.

PACS number(s): 12.38.Gc, 12.39.Hg, 13.20.He, 14.40.Nd

Typeset using REVTEX

I. INTRODUCTION

Studies of B and D meson decays shed light on many important aspects of particle physics, such as the extraction of the Cabibbo-Kobayashi-Maskawa (CKM) matrix elements, CP violation, rare decays, and hints of physics beyond the standard model. Such decays involve not only the electroweak currents, but also strong interaction dynamics in the form of hadronic matrix elements. Calculation of these matrix elements is crucial for high precision tests of the standard model.

A very promising approach to determining hadronic matrix elements from first principles in QCD is provided by numerical simulations of hadrons using lattice gauge theory. Studies of leptonic and semi-leptonic decays using lattice simulations have already been done using various techniques to handle heavy quarks on the lattice, such as the static approach [1], nonrelativistic QCD (NRQCD) [2,3], and a reformulation of conventional Wilson and clover lattice fermions [4]. In each approach, the electroweak currents must be constructed in terms of appropriate operators comprised from the gluon and quark fields of the lattice theory by calculating the renormalization factors which relate the hadronic matrix elements in the lattice-regulated theory to those in the \overline{MS} scheme. These factors are crucial for both decay constant and semi-leptonic form factor calculations. In this paper, we construct the time component of the heavy-light axial vector current in terms of operators suitable for simulations [5,6] in which the heavy quark is treated using lattice NRQCD and the light quark propagates according to the $O(a)$ -improved clover action [7], where a is the lattice spacing. The standard Wilson action is used for the gluons. This construction is carried out to one-loop order in perturbation theory and to order $1/M$, where M is the mass of the heavy quark.

The expansion of the heavy-light axial vector current in terms of appropriate lattice operators is achieved by matching relevant scattering amplitudes in perturbation theory. Consider the heavy-light pseudoscalar meson decay constant f_{PS} defined in some continuum renormalization scheme, such as \overline{MS} , by,

$$\langle 0 | A_\mu | PS(p) \rangle_{QCD} = i f_{PS} p_\mu, \quad (1)$$

where A_μ is the heavy-light axial vector current and $|PS(p)\rangle$ is a pseudoscalar meson state of momentum p . As will be seen, the axial vector current operator can be written as a sum of operators $J_{A,\text{lat}}^{(i)}$ in the lattice-regulated theory. For instance, one finds that the temporal component, $\mu = 0$, is a sum of three operators which contribute through $O(\alpha_s, 1/M, a)$, where α_s is the QCD coupling:

$$A_0 = \sum_{j=0,1,2} C_j(\alpha_s, aM) J_{A,\text{lat}}^{(j)} + O(\alpha_s^2, a^2, 1/M^2, \alpha_s a/M). \quad (2)$$

Since the role of the dimensionless coefficients C_j is to compensate for low-energy effects in the current operator from the loss of short-wavelength QCD modes in the lattice theory, one expects that, due to asymptotic freedom, they may be computed to a good approximation in perturbation theory. They are fixed by requiring that scattering amplitudes involving these current operators agree in continuum and lattice QCD to a given order in α_s , a , and $1/M$. In a perturbative determination, a process involving quarks and gluons as asymptotic states

may be used for this matching; one need not consider hadron scatterings which are much more complicated to evaluate. Note, however, that the C_j coefficients are independent of the process chosen. A one-loop evaluation of the C_j coefficients then involves the following steps: (1) select a quark-gluon scattering process induced by the heavy-light current and calculate the one-loop amplitude for this process in continuum QCD; (2) expand the amplitude in powers of $1/M$; (3) identify operators in the lattice theory that reproduce the terms in this expansion; (4) calculate the one-loop mixing matrix of these operators in the lattice theory; (5) adjust the C_j coefficients to produce a linear combination of lattice current operators whose one-loop scattering amplitude agrees with that from the \overline{MS} current to a given order in $1/M$ and a . Note that the lattice currents are matched directly to the continuum QCD currents; we do not need to use a two-step matching procedure in which the lattice currents are first matched to those in a continuum heavy-quark effective theory [8–10], which are then matched to the full QCD currents [11].

This paper is organized as follows. First, in Sec. II, we discuss various issues relevant to our matching procedure, such as the choice of expansion parameter in the perturbation series, the definition of the heavy quark mass, the regularization of infrared divergences, and the selection of a renormalization scheme. Next, a scattering process appropriate for constructing the heavy-light axial vector current in the lattice NRQCD-clover theory is chosen. We then discuss the continuum QCD calculations, and the necessary current operators in the lattice regularization scheme are identified. Sec. III describes the mixing matrix calculation in the lattice theory. The scattering amplitudes in the continuum and lattice schemes are matched in Sec. IV, and our main results, the values of the coefficients C_j for various heavy quark mass values, are presented. Renormalon ambiguities are discussed, and subtleties with infrared divergences for Wilson light quarks are pointed out.

II. CONTINUUM CALCULATION AND OPERATOR IDENTIFICATION

Our goal here is the expansion of the temporal component of the (renormalized) axial vector current in terms of (bare) operators suitable for use in lattice simulations of B and D mesons. Note that because the axial vector current is partially conserved in QCD, its operator does not actually require renormalization. This expansion is determined by matching suitable matrix elements evaluated both in continuum QCD and in the lattice theory. Since this expansion is an operator relation, the expansion coefficients are independent of the external states of the matrix elements chosen. Of course, the normalizations of the external states used in the continuum and lattice matrix elements must match in order to expose the required operator relation. Since the external states in our perturbative calculations are free quark states, this can be done at tree level by matching the normalizations of the continuum and lattice Dirac spinors (to the appropriate order in a). The use of *on-shell* wave function renormalization for both the heavy and light quark fields is then the simplest way to ensure this matching beyond tree level.

In matching the $1/M$ expansions of heavy-light matrix elements in the continuum and lattice theories, it is important to establish the relations between the quark mass parameters (both heavy and light) in each. Equality of the lattice and continuum mass parameters can be ensured in perturbation theory using the pole mass definition. The pole mass is gauge-

invariant and, within the context of perturbation theory, is a physical observable. Hence, in our calculations, we use the pole mass for M and also for the light quark mass $m = 0$. In using the pole mass definition for our quarks, we compute the continuum and lattice matrix elements using *on-shell* quark mass renormalization. Note that since the pole mass is not defined outside of perturbation theory, it is not a useful quantity for lattice simulations; the bare mass M_0 appearing in the lattice action is much more suitable. Thus, once we determine the coefficients $C_j(\alpha_s, aM)$ in terms of M , we re-express our results in terms of aM_0 using the perturbative relation between M and M_0 .

We must also know the relationship between the expansion parameters used in the continuum and lattice perturbative expressions in order to carry out the operator matching. For example, we could use $\alpha_{\overline{MS}}$ in the continuum calculations and a coupling α_V defined in terms of the momentum-space static quark potential $V(q)$ in the lattice computations. The two couplings are related by $\alpha_V = \alpha_{\overline{MS}} + O(\alpha_s^2)$. Our one loop calculations do not make use of the $O(\alpha_s^2)$ correction in the relation between the lattice and continuum expansion parameters; hence, as long as we use couplings which match at leading order, we can simply use α_s to refer to both the lattice and continuum couplings. Of course, when numerical values for the coefficients $C_j(\alpha_s, aM)$ are needed, we must specify a renormalization scheme for α_s .

The coefficients $C_j(\alpha_s, aM)$ depend on the ultraviolet regulator but contain no infrared divergences. However, our choice of on-shell mass and wave function renormalization will lead to infrared divergences at intermediate stages in our matrix element calculations. In order to demonstrate the cancellation of these divergences in the C_j coefficients, the same infrared regulator must be used in the evaluation of both the continuum and lattice matrix elements. Since the triple gluon vertex plays no role in any of our Feynman diagrams, we introduce a gluon mass λ for this purpose.

A scattering process which is suitable for our study of the heavy-light axial vector current is depicted in Fig. 1. In this process, an incoming heavy quark $|h(p)\rangle$ with momentum p scatters off a heavy-light current A_0 into an outgoing light quark $|q(p')\rangle$ with momentum p' . The axial-vector current operator is given by $A_\mu(x) = \bar{q}(x) \hat{\gamma}_5 \hat{\gamma}_\mu h(x)$ in terms of the light quark field $q(x)$ and the heavy quark field $h(x)$. The first step in our study is the calculation of the amplitude for this continuum-QCD process to one-loop order in perturbation theory. Using the on-shell mass and wave function renormalization scheme in Feynman gauge and expanding in $1/M$ (except for the Dirac spinor of the heavy quark), one finds

$$\begin{aligned} \langle q(p') | A_0 | h(p) \rangle_{QCD} = & a_1 \left[\bar{u}_q(p') \hat{\gamma}_5 \hat{\gamma}_0 u_h(p) \right] + a_2 \left[\frac{p_0}{M} \bar{u}_q(p') \hat{\gamma}_5 u_h(p) \right] \\ & + a_3 \left[\frac{p \cdot p'}{M^2} \bar{u}_q(p') \hat{\gamma}_5 \hat{\gamma}_0 u_h(p) \right] + a_4 \left[\frac{p'_0}{M} \bar{u}_q(p') \hat{\gamma}_5 u_h(p) \right] \\ & + a_5 \left[\frac{p \cdot p'}{M^2} \frac{p_0}{M} \bar{u}_q(p') \hat{\gamma}_5 u_h(p) \right] + O(1/M^2), \end{aligned} \quad (3)$$

with

$$\begin{aligned} a_1 &= 1 + \frac{\alpha_s}{3\pi} \left[3 \ln \frac{M}{\lambda} - \frac{11}{4} \right], \\ a_2 &= \frac{\alpha_s}{3\pi} 2, \end{aligned}$$

$$\begin{aligned}
a_3 &= \frac{\alpha_s}{3\pi} \left[6 \ln \frac{M}{\lambda} - \frac{8\pi}{3} \frac{M}{\lambda} + \frac{1}{2} \right], \\
a_4 &= \frac{\alpha_s}{3\pi} \left[-2 \ln \frac{M}{\lambda} + \frac{1}{2} \right], \\
a_5 &= \frac{\alpha_s}{3\pi} \left[-4 \ln \frac{M}{\lambda} + 5 \right],
\end{aligned} \tag{4}$$

where $u_h(p)$ and $u_q(p')$ are the standard spinors for the heavy and light quarks, respectively, which satisfy the Dirac equation. The light quark mass is set equal to zero. Our conventions for the Dirac $\hat{\gamma}$ -matrices in Minkowski space are given in the appendix. Ultraviolet divergences are regulated using dimensional regularization and fully anti-commuting $\hat{\gamma}_5$ matrices are used. As previously mentioned, we use a gluon mass λ in order to regulate infrared divergences. The three diagrams which contribute to this amplitude at one-loop order are shown in Fig. 1.

In lattice NRQCD, the heavy quark is described in terms of a two-component (in spin space) field $\psi(x)$. The Dirac field $h(x)$ is related to ψ (and the antiquark field $\bar{\psi}$) by a unitary Foldy-Wouthuysen transformation [12],

$$h(x) = U_{FW}^{-1} \begin{pmatrix} \psi(x) \\ \tilde{\psi}(x) \end{pmatrix}. \tag{5}$$

This transformation decouples the upper and lower components of the Dirac field, thereby separating the quark field from the antiquark field. To facilitate the identification of lattice NRQCD operators capable of matching Eq. 3, we similarly transform the external state spinor $u_h(p)$ (with normalization $u_h^\dagger u_h = 1$) into a nonrelativistic Pauli spinor:

$$u_h(p) = \left[1 - \frac{1}{2M} (\hat{\gamma} \cdot \mathbf{p}) \right] u_Q(p) + O(1/M^2), \tag{6}$$

where

$$u_Q(p) = \begin{pmatrix} U_Q \\ 0 \end{pmatrix}, \tag{7}$$

and U_Q is a two-component external state spinor depending only on the spin of the heavy quark. Using Eq. 6, the relation $\hat{\gamma}_0 u_Q(p) = u_Q(p)$, and the Dirac equation for the light quark $\bar{u}_q(p') p'_0 = \bar{u}_q(p') \hat{\gamma} \cdot \mathbf{p}' \hat{\gamma}_0$, Eq. 3 may be written

$$\langle q(p') | A_0 | h(p) \rangle_{QCD} = \eta_0^A \hat{\Omega}_0 + \eta_1^A \hat{\Omega}_1 + \eta_2^A \hat{\Omega}_2 + O(\alpha_s^2, 1/M^2), \tag{8}$$

where $\Gamma = \hat{\gamma}_5 \hat{\gamma}_0$, and

$$\hat{\Omega}_0 = \bar{u}_q(p') \Gamma u_Q(p), \tag{9}$$

$$\hat{\Omega}_1 = -\bar{u}_q(p') \Gamma \frac{\hat{\gamma} \cdot \mathbf{p}}{2M} u_Q(p), \tag{10}$$

$$\hat{\Omega}_2 = -\bar{u}_q(p') \frac{\hat{\gamma} \cdot \mathbf{p}'}{2M} \Gamma u_Q(p). \tag{11}$$

The coefficients in Eq. 8 may be written

$$\begin{aligned}
\eta_0^A &= (a_1 + a_2) = 1 + \alpha_s \tilde{B}_0, \\
\eta_1^A &= (a_1 - a_2) = 1 + \alpha_s \tilde{B}_1, \\
\eta_2^A &= 2(a_3 + a_4 + a_5) = \alpha_s \tilde{B}_2,
\end{aligned} \tag{12}$$

where

$$\begin{aligned}
\tilde{B}_0 &= \frac{1}{3\pi} \left[3 \ln \frac{M}{\lambda} - \frac{3}{4} \right], \\
\tilde{B}_1 &= \frac{1}{3\pi} \left[3 \ln \frac{M}{\lambda} - \frac{19}{4} \right], \\
\tilde{B}_2 &= \frac{1}{3\pi} \left[12 - \frac{16\pi}{3} \frac{M}{\lambda} \right].
\end{aligned} \tag{13}$$

Having obtained the $1/M$ expansion of the above scattering amplitude in continuum QCD, the next step is to identify operators in the lattice theory which can reproduce the terms in this expansion. An inspection of Eq. 8 suggests immediately that matrix elements of the following three lattice operators should be considered:

$$J_{A,\text{lat}}^{(0)}(x) = \bar{q}(x) \Gamma Q(x), \tag{14}$$

$$J_{A,\text{lat}}^{(1)}(x) = \frac{-1}{2M_0} \bar{q}(x) \Gamma \boldsymbol{\gamma} \cdot \boldsymbol{\nabla} Q(x), \tag{15}$$

$$J_{A,\text{lat}}^{(2)}(x) = \frac{1}{2M_0} \bar{q}(x) \boldsymbol{\gamma} \cdot \overleftarrow{\boldsymbol{\nabla}} \Gamma Q(x), \tag{16}$$

where $q(x)$ is now the light quark field in the lattice theory, M_0 is the bare heavy quark mass, and $Q(x)$ is related to the heavy quark field $\psi(x)$ in lattice NRQCD by

$$Q(x) = \begin{pmatrix} \psi(x) \\ 0 \end{pmatrix}. \tag{17}$$

We use the bare quark mass M_0 in the above definitions since it is the natural mass to use in lattice simulations and because the pole mass M is not well defined beyond perturbation theory. The covariant finite difference operators ∇_μ and $\overleftarrow{\nabla}_\mu$ are defined as usual in terms of the link variables $U_\mu(x)$ which are the parallel transport operators from sites x to neighboring sites $x+a_\mu$ in the gauge field. The definitions of these operators are given below, along with other derivative operators which will be needed later:

$$a\nabla_\mu O(x) = \frac{1}{2u_0} [U_\mu(x)O(x+a_\mu) - U_\mu^\dagger(x-a_\mu)O(x-a_\mu)], \tag{18}$$

$$O(x) a\overleftarrow{\nabla}_\mu = \frac{1}{2u_0} [O(x+a_\mu)U_\mu^\dagger(x) - O(x-a_\mu)U_\mu(x-a_\mu)], \tag{19}$$

$$a^2 \Delta^{(2)} O(x) = \sum_{k=1}^3 \left(u_0^{-1} [U_k(x)O(x+a_k) + U_k^\dagger(x-a_k)O(x-a_k)] - 2O(x) \right), \tag{20}$$

$$a^2 \nabla^{(2)} O(x) = \sum_{\mu=0}^3 \left(u_0^{-1} [U_\mu(x)O(x+a_\mu) + U_\mu^\dagger(x-a_\mu)O(x-a_\mu)] - 2O(x) \right), \tag{21}$$

where $O(x)$ is an operator defined at lattice site x with appropriate color structure, and u_0 is the mean link parameter introduced by the tadpole improvement procedure [13]. Note that these lattice operators are defined in Euclidean space; our Euclidean space conventions are outlined in the appendix.

III. LATTICE CALCULATION

In this section, we describe the one-loop calculation in the lattice theory of the mixing matrix Z_{ij} defined by

$$\langle q(p') | J_{A,\text{lat}}^{(i)} | h(p) \rangle_{\text{lat}} = \sum_j Z_{ij} \Omega_j + O(\alpha_s^2, 1/M^2, a^2, \alpha_s a/M), \quad (22)$$

where Ω_j are the Euclidean-space counterparts of the $\hat{\Omega}_j$ defined in Eqs. 9-11. First, the lattice actions used in these calculations are specified. The necessary Feynman diagrams are then presented, and their evaluation in lattice perturbation theory is outlined.

For the heavy quark, we use the following NRQCD action density [2]:

$$a\mathcal{L}_{\text{NRQCD}} = \psi^\dagger(x) \psi(x) - \psi^\dagger(x+a_t) \left(1 - \frac{a\delta H}{2}\right) \left(1 - \frac{aH_0}{2n}\right)^n \frac{U_4^\dagger(x)}{u_0} \left(1 - \frac{aH_0}{2n}\right)^n \left(1 - \frac{a\delta H}{2}\right) \psi(x), \quad (23)$$

where

$$H_0 = -\frac{\Delta^{(2)}}{2M_0}, \quad (24)$$

$$\delta H = -c_B \frac{g}{2M_0} \boldsymbol{\sigma} \cdot \mathbf{B}. \quad (25)$$

The positive integer n is introduced to stabilize the highest momentum modes in the heavy quark propagator [2]; the condition, $n > 3/aM_0$, has proven to be a reliable guide. Note that the above NRQCD action does not include the heavy quark mass term. The QCD coupling g is related to α_s in the usual manner, $\alpha_s = g^2/(4\pi)$, and σ_j are the standard Pauli spin matrices. At tree level, $c_B = 1$; the one-loop contribution to c_B is an $O(\alpha_s^2)$ effect in our mixing matrix calculation and hence can be ignored here. The chromomagnetic field is given by $B_j(x) = -\frac{1}{2}\epsilon_{jlm}F_{lm}(x)$, where the Hermitian and traceless field strength tensor $F_{\mu\nu}(x)$ is defined at the sites of the lattice in terms of clover-leaf operators:

$$\begin{aligned} F_{\mu\nu}(x) &= \mathcal{F}_{\mu\nu}(x) - \frac{1}{3}\text{Tr}\mathcal{F}_{\mu\nu}(x), \\ \mathcal{F}_{\mu\nu}(x) &= \frac{-i}{2a^2g} \left(\Omega_{\mu\nu}(x) - \Omega_{\mu\nu}^\dagger(x) \right), \\ \Omega_{\mu\nu}(x) &= \frac{1}{4u_0^4} \sum_{\{(\alpha,\beta)\}_{\mu\nu}} U_\alpha(x) U_\beta(x+a_\alpha) U_{-\alpha}(x+a_\alpha+a_\beta) U_{-\beta}(x+a_\beta), \end{aligned} \quad (26)$$

with $\{(\alpha,\beta)\}_{\mu\nu} = \{(\mu,\nu), (\nu,-\mu), (-\mu,-\nu), (-\nu,\mu)\}$ for $\mu \neq \nu$.

For the light quarks, we use the clover action [7],

$$a\mathcal{L}_{light} = \bar{q} \not{\nabla} q - a \frac{r}{2} \bar{q} \nabla^{(2)} q + m_0 \bar{q} q - i g a \frac{r}{4} \sum_{\mu, \nu} \bar{q} \sigma_{\mu \nu} F_{\mu \nu} q, \quad (27)$$

where $\not{\nabla} = \sum_{\mu} \gamma_{\mu} \nabla_{\mu}$, m_0 is the bare light quark mass, $\sigma_{\mu \nu} = \frac{1}{2} [\gamma_{\mu}, \gamma_{\nu}]$, and we set the Wilson parameter $r = 1$. The one-loop correction to the clover coefficient is an $O(\alpha_s^2)$ effect in our matching calculation and can be neglected.

Lattice perturbation theory calculations are much more laborious than those in continuum perturbation theory. Not only do more diagrams contribute to a given process, but the complicated functional forms of the propagators and vertex functions (presented in the appendix) necessitate the use of numerical methods in evaluating the integrals over internal loop momenta. For the scattering process considered here, there are five additional one-loop Feynman diagrams in the lattice theory: three are vertex corrections, shown in Fig. 2, and two are extra external leg corrections, shown in Fig. 3. The Feynman rules are determined by expanding the total lattice action in terms of g using

$$U_{\mu}(x) \equiv \exp \left[i a g G_{\mu} \left(x + \frac{a_{\mu}}{2} \right) \right], \quad (28)$$

and $u_0 = 1 - \alpha_s u_0^{(2)} + O(\alpha_s^2)$, then Fourier transforming into momentum space. $G_{\mu}(x)$ is the lattice gluon field defined at the midpoints of the links connecting neighboring sites.

We calculate the amplitudes corresponding to the Feynman diagrams of Figs. 1-3 in two very different ways and verify that the results agree. In the first method, all spin matrix manipulations and derivatives with respect to external momenta are done by hand. The resulting integrals are also simplified by hand, including the subtraction of terms to remove infrared divergences. The remaining infrared-finite integrals are then done numerically using Monte Carlo and adaptive Gaussian quadrature techniques.

In the second method, nearly all aspects of the calculation are automated. First, the propagators and vertex functions are expressed as functions in C++ whose arguments are the appropriate four momenta implemented using a class **fourvec**. Spin algebra is accomplished using explicit matrix representations; this is done by defining new class structures in C++, such as **pauli** and **dirac**, and overloading all of the necessary arithmetic operators for ease of use. Derivatives with respect to external momenta are taken using automatic differentiation [14]. This is implemented by defining in C++ a class **Tcomplex** which carries out the multivariate Taylor series expansions. A variable of type **Tcomplex** is treated by the end user just as if it were a regular complex scalar variable since all appropriate arithmetic operators and mathematical functions are overloaded. However, a **Tcomplex** variable is actually an array containing the function value and all of its derivatives up to some order; an indexing member function is used to return a specific term in the Taylor series expansion. All derivatives are taken automatically using analytical techniques; the end user never needs to write subroutines for taking these derivatives.

The above tools allow one to easily write C++ functions to compute the integrands for all of our one-loop Feynman diagrams. The integrals corresponding to the graphs in Figs. 2 and 3 are easily evaluated using Monte Carlo techniques. We use the integration routine **VEGAS** [15]. Note that, in lattice perturbation theory, each internal loop momentum k is

restricted to the first Brillouin zone $-\pi < ak_\mu \leq \pi$. However, due to infrared divergences, the other integrals cannot be directly calculated. We evaluate these integrals in a sequence of steps. First, we subtract from the lattice integrand $I_{\text{lat}}(k)$, where k is the loop momentum, the analogous integrand from the continuum theory, $I_{\text{con}}(k)$. The integral of this difference over the first Brillouin zone is infrared finite and can be evaluated using the Monte Carlo method. We then multiply the continuum integrand by a factor $f(k)$ to render the integral insensitive to the shape of the first Brillouin zone. This factor must also be chosen such that the integral of $[1-f(k)] I_{\text{con}}(k)$ is infrared finite. For example, $f(k) = \exp(-\rho k^2)$ where $\rho = \pi/2$ is often a good choice. We then use the Monte Carlo method to evaluate the integral of $[1-f(k)] I_{\text{con}}(k)$. The infrared divergence has then been isolated in the integral of $f(k) I_{\text{con}}(k)$. Since $f(k)$ is chosen to remove any appreciable sensitivity of the integral to the edge of the Brillouin zone, we can change to hyperspherical coordinates and integrate over the interior of an infinitely large sphere to a good approximation. This simplifies the calculation and allows us to easily identify and analytically manipulate the infrared divergent pieces of the integrand.

Using these two methods, we obtain results for the mixing matrix Z_{ij} in Eq. 22, again using the on-shell renormalization scheme in Feynman gauge. Note that the nonrelativistic external-state spinors $u_Q(p)$ are identical in the lattice and continuum theories. For the clover action, the external light-quark spinors $u_q(p')$ differ only at $O(a^2)$. At one-loop, the mixing matrix elements may be written

$$Z_{ij} = \delta_{ij} + \alpha_s \left[\frac{1}{2} (\tilde{C}_q + \tilde{C}_Q) \delta_{ij} + \tilde{C}_m \delta_{i1} \delta_{j1} + \tilde{\zeta}_{ij} \right], \quad (29)$$

where \tilde{C}_q and \tilde{C}_Q are the contributions from the light- and heavy-quark external leg corrections (that is, from wave function renormalization factors), and $\tilde{\zeta}_{ij}$ denote the contributions from the vertex corrections. Our use of an on-shell renormalization scheme with lattice operators defined in terms of the bare mass M_0 is responsible for the term proportional to \tilde{C}_m , where

$$M = [1 + \alpha_s \tilde{C}_m] M_0 + O(\alpha_s^2). \quad (30)$$

Note that although the current operators $J_{A,\text{lat}}^{(i)}$ are defined using M_0 , the pole mass M must appear in Ω_j . The factors in Eq. 29 may be further decomposed:

$$\begin{aligned} \tilde{C}_q &= C_q + \frac{2}{3\pi} \ln a\lambda + C_q^{\text{TI}}, \\ \tilde{C}_Q &= C_Q - \frac{4}{3\pi} \ln a\lambda, \\ \tilde{C}_m &= C_m + C_m^{\text{TI}}, \\ \tilde{\zeta}_{ij} &= \zeta_{ij} + \zeta_{ij}^{\text{TI}} + \zeta_{ij}^{\text{IR}}, \end{aligned} \quad (31)$$

where C_q , C_Q , C_m , and ζ_{ij} are infrared finite and independent of the tadpole improvement factor u_0 , and ζ_{ij}^{IR} and ζ_{ij}^{TI} contain the infrared divergences and tadpole improvement contributions, respectively, from the vertex corrections. Contributions to \tilde{C}_q and \tilde{C}_m from the tadpole improvement counterterms are denoted by C_q^{TI} and C_m^{TI} , respectively.

IV. RESULTS

To complete the operator matching, we transform Eq. 8 from Minkowski to Euclidean space, use Eqs. 22 and 29, then peel off the dependence on the external states. This yields the following operator relation:

$$\begin{aligned} A_0 = & \left(1 + \alpha_s \left[\tilde{B}_0 - \frac{1}{2}(\tilde{C}_q + \tilde{C}_Q) - \tilde{\zeta}_{00} - \tilde{\zeta}_{10} \right] \right) J_{A,\text{lat}}^{(0)} \\ & + \left(1 + \alpha_s \left[\tilde{B}_1 - \frac{1}{2}(\tilde{C}_q + \tilde{C}_Q) - \tilde{C}_m - \tilde{\zeta}_{01} - \tilde{\zeta}_{11} \right] \right) J_{A,\text{lat}}^{(1)} \\ & + \alpha_s \left[\tilde{B}_2 - \tilde{\zeta}_{02} - \tilde{\zeta}_{12} \right] J_{A,\text{lat}}^{(2)} + O(\alpha_s^2, a^2, 1/M^2, \alpha_s a/M). \end{aligned} \quad (32)$$

As expected, we find that the infrared divergences from the various terms in the expansion coefficients cancel. We now have the desired expansion coefficients C_j of Eq. 2 in terms of the pole mass M . As previously mentioned, the bare mass M_0 is a much more convenient mass parameter. Our results are easily expressed in terms of aM_0 using Eq. 30, which, in this case, simply amounts to replacing M by M_0 :

$$\begin{aligned} A_0 = & \left(1 + \alpha_s \left[B_0 - \frac{1}{2}(C_q + C_q^{\text{TI}} + C_Q) - \tau_0 \right] \right) J_{A,\text{lat}}^{(0)} \\ & + \left(1 + \alpha_s \left[B_1 - \frac{1}{2}(C_q + C_q^{\text{TI}} + C_Q) - C_m - C_m^{\text{TI}} - \tau_1 - \tau_1^{\text{TI}} \right] \right) J_{A,\text{lat}}^{(1)} \\ & + \alpha_s [B_2 - \tau_2] J_{A,\text{lat}}^{(2)} + O(\alpha_s^2, a^2, 1/M^2, \alpha_s a/M), \end{aligned} \quad (33)$$

where $B_0 = \ln(aM_0)/\pi - 1/(4\pi)$, $B_1 = \ln(aM_0)/\pi - 19/(12\pi)$, $B_2 = 4/\pi$, $\tau_0 = \zeta_{00} + \zeta_{10}$, $\tau_1 = \zeta_{01} + \zeta_{11}$, and $\tau_2 = \zeta_{02} + \zeta_{12}$. The factors arising from tadpole improvement counterterms are given by

$$\begin{aligned} C_q^{\text{TI}} &= -u_0^{(2)}, \\ C_m^{\text{TI}} &= -u_0^{(2)} \left(1 - \frac{3}{2 n a M_0} \right), \\ \tau_1^{\text{TI}} &= u_0^{(2)}. \end{aligned} \quad (34)$$

For the usual plaquette definition $u_0 = \langle \frac{1}{3} \text{Tr} U_{\square} \rangle^{1/4}$ in the Wilson gluonic action, $u_0^{(2)} = \pi/3$. For massless clover quarks, $C_q = 1.030$. Results for τ_0 , τ_1 , τ_2 , C_Q and C_m for various values of aM_0 are listed in Table I.

Explicit calculation reveals that τ_2 behaves as $-2aM_0\zeta_{disc}$ as M_0 becomes large, where ζ_{disc} is found numerically to be $\zeta_{disc} = 1.00(1)$. This factor can be viewed as arising from a discretization correction $J_{A,\text{lat}}^{(disc)}$ to $J_{A,\text{lat}}^{(0)}$,

$$J_{A,\text{lat}}^{(disc)} = a \bar{q}(x) \boldsymbol{\gamma} \cdot \bar{\nabla} \Gamma Q(x), \quad (35)$$

analogous to the $O(a)$ correction $a \partial_\mu P$, where P is the pseudoscalar density, to the axial current in light-light quark systems [16]. We can then define an *improved* current operator

$$J_{A,\text{lat}}^{(0)imp} = J_{A,\text{lat}}^{(0)} + C_A J_{A,\text{lat}}^{(disc)}, \quad (36)$$

where we write

$$C_A = \alpha_s \left(1 + \frac{\zeta_A}{2aM_0} \right). \quad (37)$$

This decomposition is not unique, and hence, we leave ζ_A as a free parameter. Different choices of ζ_A lead to different $O(\alpha_s^2)$ contributions being included in Eq. 33. Taking this into consideration, Eq. 33 can be written

$$A_0 = (1 + \alpha_s \rho_0) J_{A,\text{lat}}^{(0)\text{imp}} + (1 + \alpha_s \rho_1) J_{A,\text{lat}}^{(1)} + \alpha_s (\rho_2 - \zeta_A) J_{A,\text{lat}}^{(2)} + O(\alpha_s^2, a^2, 1/M^2, \alpha_s a/M), \quad (38)$$

so that the C_j coefficients of Eq. 2 become $C_0 = 1 + \alpha_s \rho_0$, $C_1 = 1 + \alpha_s \rho_1$, and $C_2 = \alpha_s (\rho_2 - \zeta_A)$. This equation is our final result. Note that at $O(\alpha_s)$, the ζ_A dependence in $J_{A,\text{lat}}^{(0)\text{imp}}$ cancels that in $C_2 J_{A,\text{lat}}^{(2)}$. Numerical results for ρ_0 , ρ_1 , and ρ_2 are given in Table II.

In Ref. [6], B meson decay constants were computed in simulations in which the heavy quark propagation was described by an NRQCD action different from Eq. 23; in particular, higher order corrections were included. The values of ρ_0 , ρ_1 , and ρ_2 for the action used in these simulations are given in Table III.

In order to use Eq. 38 in a simulation, a value for α_s must be specified. To do this, one must first choose a renormalization scheme for α_s ; in the case of a running coupling, a means of setting the scale must then be devised; lastly, the value of the coupling at some reference scale must be determined. A coupling $\alpha_V(q^*)$ defined in terms of the short-distance static potential with a scale-setting prescription based on the mean value theorem is advocated in Ref. [13]; the value of $\alpha_V(3.402/a)$ can be obtained from measurements of the average plaquette. Unfortunately, we have not computed the q^* scales for the ρ_0 , ρ_1 , and ρ_2 coefficients. However, based on findings in Refs. [8] and [17], we expect that $q^* \sim 2/a$. An alternative choice for the expansion parameter is a non-running boosted coupling $\alpha_b = 6/(4\pi\beta u_0^4)$; the value of this coupling is typically comparable to $\alpha_V(\pi/a)$.

For the range of aM_0 values considered here, our results show no evidence that perturbation theory is failing. From Tables II and III, one sees that the one-loop corrections to C_0 are very small. Values for ρ_0 are typically near -0.3 for all aM_0 considered; multiplying by $\alpha_s \sim 0.2$ yields one-loop corrections to C_0 which are approximately 5% of the tree-level contribution. For the large range of aM_0 values studied, ρ_1 varies between -0.7 and 0.5 ; hence, one-loop corrections to C_1 are never larger than about 15%. The magnitudes of the values for ρ_2 are significantly larger than those for ρ_0 and ρ_1 . If we set $\zeta_A = 0$, then $C_A = \alpha_s$ and $C_2 = \alpha_s \rho_2$ which, using $\alpha_s \sim 0.2$, varies between 0.2 and 0.9 for the range of aM_0 values studied here. Since C_2 has no tree-level contribution, at least a two-loop result is needed to check the convergence of its perturbative expansion.

As in all applications of perturbative QCD, nonperturbative contributions to C_j are possible. For example, the perturbative expansions of the C_j coefficients contain renormalon ambiguities arising from a slight mismatch between the infrared physics of the lattice theory and that of continuum QCD. This mismatch is caused by discretization artifacts and the truncation of the $1/M$ expansion. In our calculation, contributions coming from momenta small relative to a given infrared scale $q_0 \ll 1/a, M$ are all suppressed by $a^2 q_0^2$ or q_0^2/M^2

since the infrared structure of our lattice theory is designed to agree with continuum QCD through $O(a, 1/M)$. This infrared suppression is not true diagram-by-diagram (some diagrams are even infrared divergent), but the infrared contribution is suppressed by a^2 or $1/M^2$ when all diagrams are summed. For example, in some analyses [18], coefficients like C_0 are separated into the contribution c_0 from the leading operator (here $J_{A,\text{lat}}^{(0)}$) and contributions \tilde{c}_0 from mixings with higher-dimension operators (here $J_{A,\text{lat}}^{(1)}$ and $J_{A,\text{lat}}^{(2)}$). In our analysis, such a separation is artificial and would be a mistake since it induces $O(a, 1/M)$ ambiguities in the separate pieces c_0 and \tilde{c}_0 . These ambiguities cancel when the pieces are recombined, leaving contributions to C_0 suppressed by $a^2 q_0^2$ or q_0^2/M^2 . Thus, any renormalon ambiguities are suppressed by the same factors and are at worst comparable to the other truncation errors in the analysis.

Our calculation differs from conventional lattice calculations in that the a^2 truncation errors, perturbative and nonperturbative, cannot be made arbitrarily small by reducing the lattice spacing [2]. This is because NRQCD has nonrenormalizable interactions whose couplings do not vanish as $a \rightarrow 0$. The perturbative expansions for C_j have power-law terms of the form $\alpha_s/(aM)^n$ which ruin the convergence of perturbation theory if a is taken to zero. In practice, this problem is avoided by keeping the lattice spacing large enough that $1/(aM)$ never becomes large. Our inability to take $a \rightarrow 0$ in NRQCD fundamentally limits the precision of our $O(a, 1/M)$ accurate formalism. If improved precision is needed, we must reduce the truncation errors by using more accurate discretizations of the lattice currents and action. In this way truncation errors, renormalon ambiguities, etc. are pushed off to $O(a^3, 1/M^2)$ or higher.

The results in Table II are suitable for values of aM_0 appropriate for current simulations of heavy-light systems using NRQCD. However, terms proportional to $\ln(aM_0)$ cause the $O(\alpha_s)$ contributions to C_0 and C_1 to become large as aM_0 becomes large. In such cases, the renormalization group should be used to improve upon the estimates from one-loop perturbation theory. Since the left-hand side of Eq. 2 is independent of the lattice spacing, it follows that, neglecting $O(a^2)$ terms,

$$a \frac{d}{da} \left[\sum_k C_k(\alpha_s, aM_0) \langle J_{A,\text{lat}}^{(k)} \rangle \right] = 0. \quad (39)$$

Using Eq. 22 and $d\Omega_j/da = 0$, a renormalization group equation for the C_j coefficients, collected into a vector \vec{C} , can be obtained which describes the change in C_j as the lattice spacing is varied:

$$\left(a \frac{d}{da} + \gamma^{\text{tr}} \right) \vec{C} = 0, \quad (40)$$

where the anomalous dimension matrix is given by

$$\gamma_{ij}(\alpha_s, aM_0) = \sum_k \left(a \frac{d}{da} Z_{ik} \right) Z_{kj}^{-1}. \quad (41)$$

In the limit of large aM_0 , we find $\gamma = \text{diag}(-\alpha_s/\pi, -\alpha_s/\pi, 0)$ and Eq. 40 can be easily solved. First, express the C_j coefficients as a function of $\alpha_s(a)$ and aM instead of $\alpha_s(a)$ and

$aM_0(a)$ since M is fixed and does not run with a . If the lattice theory is renormalized in such a way that the renormalization group β -function $\beta_{\text{RG}} = -a d\alpha_s(a^{-1})/da$ is independent of M_0 and m_0 , then

$$\beta_{\text{RG}}(\alpha_s) = -2\beta_0 \alpha_s^2 - 2\beta_1 \alpha_s^3 + O(\alpha_s^4), \quad (42)$$

where $\beta_0 = (11 - \frac{2}{3}N_f)/(4\pi)$ and $\beta_1 = (102 - \frac{38}{3}N_f)/(16\pi^2)$, for N_f light quark flavors. For large, fixed M , Eq. 40 then tells us that the change in C_0 and C_1 in going from an initial lattice spacing a_1 to a smaller lattice spacing a_2 is given, in leading logarithmic approximation, by

$$\frac{C_i(a_2 M)}{C_i(a_1 M)} = \left[\frac{\alpha_s(1/a_2)}{\alpha_s(1/a_1)} \right]^{1/(2\beta_0\pi)}, \quad (43)$$

for $i = 0, 1$, where $\alpha_s(\mu)$ is the familiar QCD running coupling; its two-loop form is

$$\alpha_s(\mu) = \left[\beta_0 \ln(\mu^2/\Lambda^2) + \frac{\beta_1}{\beta_0} \ln \ln(\mu^2/\Lambda^2) \right]^{-1}. \quad (44)$$

Let $a_2 M = a M'_0$ and $a_1 M = a M_0$, then

$$\begin{aligned} \frac{\alpha_s(1/a_2)}{\alpha_s(1/a_1)} &= 1 - \alpha_s \beta_0 \ln \left(\frac{a_1^2}{a_2^2} \right) + O(\alpha_s^2), \\ &= 1 - \alpha_s \beta_0 \ln \left(\frac{M_0^2}{M'_0} \right) + O(\alpha_s^2), \\ &= \frac{\alpha_s(M_0)}{\alpha_s(M'_0)} + O(\alpha_s^2). \end{aligned} \quad (45)$$

Hence, to the order at which we are working, Eq. 43 is equivalent to

$$\frac{C_i(a M'_0)}{C_i(a M_0)} = \left[\frac{\alpha_s(M'_0)}{\alpha_s(M_0)} \right]^{-1/(2\beta_0\pi)}, \quad (46)$$

for large $a M_0$ and $a M'_0$. When $a M_0$ is not large, the dependence of γ_{ij} on $a M_0$ cannot be neglected and Eq. 46 must be suitably modified.

As an aside, we mention the following fact. If one wishes to use the Wilson action instead of the clover action for the light quark, one cannot include the discretization correction term $J_{A,\text{lat}}^{(\text{disc})}$. If one includes $J_{A,\text{lat}}^{(\text{disc})}$ while using Wilson light quarks, one finds an uncancelled logarithmic infrared divergence upon attempting to match the continuum and lattice scattering amplitudes. This divergence is removed by including contributions from the $O(a)$ -correction term in the clover action.

V. SUMMARY

In this paper, the temporal component of the heavy-light axial vector current A_μ was expanded in terms of lattice operators suitable for use in simulations of B and D mesons.

The expansion was carried out to $O(1/M)$ by matching relevant scattering amplitudes to one-loop order in perturbation theory. The (massless) light quark was described in the lattice theory using the $O(a)$ -improved clover action of Eq. 27, and the NRQCD action of Eq. 23 was used to treat the heavy quark. The standard Wilson action was used for the lattice gluons. The expansion of the heavy-light current was found to be

$$A_0 = C_0 J_{A,\text{lat}}^{(0)\text{imp}} + C_1 J_{A,\text{lat}}^{(1)} + C_2 J_{A,\text{lat}}^{(2)} + O(\alpha_s^2, a^2, 1/M^2, \alpha_s a/M), \quad (47)$$

where the lattice operators are defined in Eqs. 14, 15, 16, and 36, and $C_0 = 1 + \alpha_s \rho_0$, $C_1 = 1 + \alpha_s \rho_1$, $C_2 = \alpha_s(\rho_2 - \zeta_A)$ and $C_A = \alpha_s[1 + \zeta_A/(2aM_0)]$. Values for ρ_0 , ρ_1 , and ρ_2 are listed in Table II for various bare heavy quark masses. ζ_A remains as a free parameter; different choices for the value of ζ_A lead to different $O(\alpha_s^2)$ contributions being included in Eq. 47. The one-loop corrections for C_0 and C_1 were shown to be small relative to the tree-level contributions for the range of aM_0 studied; no evidence of a breakdown in perturbation theory was found. Since C_2 has no tree-level contribution, at least a two-loop calculation would be needed to check the behavior of its perturbative expansion. Renormalon ambiguities were argued to be at worst of the same order as our other systematic errors.

Our results have already been used in B -meson simulations [5] measuring f_B . More recently, B meson decay constants were computed [6] in simulations using an NRQCD action with higher-order interactions not included in Eq. 23; the values of ρ_0 , ρ_1 , and ρ_2 for the action used in these simulations are given in Table III. In the future, we plan to apply the methods described in this paper to the expansion of other currents, such as the vector current, in terms of appropriate lattice operators.

VI. ACKNOWLEDGMENTS

We would like to thank Peter Lepage, Arifa Ali Khan, Tanmoy Bhattacharya, and Geoff Bodwin for helpful discussions. We would also like to thank Christine Davies for checking some of our continuum QCD calculations. This work was supported by the U.S. DOE, Grants No. DE-FG03-90ER40546 and DE-FG02-91ER40690, and by NATO grant CRG 941259.

APPENDIX A: FEYNMAN RULES

The NRQCD and light quark actions are given in Eqs. 23 and 27 in Sec. III. The Feynman rules of perturbation theory can be derived from these actions using, for instance, the methods of Ref. [19]. Most of the rules relevant for the calculations of this article are collected in this appendix. Various conventions used in our computations are also outlined. To simplify notation, we set the lattice spacing $a = 1$ in this appendix.

Minkowski-space quantities are indicated either by a caret, such as $\hat{\gamma}$, or by a subscript or superscript (M) , such as $x_j^{(M)}$. The metric tensor in Minkowski space is taken to be $g_{\mu\nu} = \text{diag}(1, -1, -1, -1)$ and the Dirac matrices satisfy $\{\hat{\gamma}_\mu, \hat{\gamma}_\nu\} = 2 g_{\mu\nu}$. We use the Dirac-Pauli representation:

$$\begin{aligned}\hat{\gamma}^0 &= \hat{\gamma}_0 = \begin{pmatrix} I & 0 \\ 0 & -I \end{pmatrix}, \\ \hat{\gamma}^j &= -\hat{\gamma}_j = \begin{pmatrix} 0 & \sigma_j \\ -\sigma_j & 0 \end{pmatrix},\end{aligned}$$

where σ_j are the standard Pauli spin matrices. Also, we define $\hat{\gamma}_5 = i\hat{\gamma}^0\hat{\gamma}^1\hat{\gamma}^2\hat{\gamma}^3$.

Euclidean-space four-vectors are defined in terms of Minkowski-space four-vectors using $x_0 = x^0 = i x_{(M)}^0$ and $x_j = x^j = x_{(M)}^j = -x_j^{(M)}$, for $j = 1, 2, 3$. For the derivative operator, $\partial_0 = \partial^0 = -i\partial_0^{(M)}$ and $\partial_j = \partial^j = \partial_j^{(M)} = -\partial_{(M)}^j$. Note that the gauge field $G_{(M)}^\mu = (\phi_{(M)}, \vec{G}_{(M)})$ Wick-rotates into Euclidean space as a covariant vector, as does the gauge-covariant derivative $D_{(M)}^\mu$. The Euclidean-space Dirac matrices satisfy $\{\gamma_\mu, \gamma_\nu\} = 2\delta_{\mu\nu}$ and are related to their Minkowski-space counterparts by $\gamma_0 = \gamma^0 = \hat{\gamma}^0$, $\gamma_j = \gamma^j = -i\hat{\gamma}^j = i\hat{\gamma}_j$, and $\gamma_5 = \gamma_0\gamma_1\gamma_2\gamma_3 = \hat{\gamma}_5$. Also, $\sigma_{\nu\mu} \equiv \frac{1}{2}[\gamma_\nu, \gamma_\mu]$. To be consistent with our conventions for Euclidean-space γ matrices, we define Euclidean-space quark-bilinear axial and vector currents by $A_0 = A_0^{(M)}$, $A^j = -iA_{(M)}^j$, $V_0 = V_0^{(M)}$, and $V^j = -iV_{(M)}^j$. The chromoelectric and chromomagnetic fields are defined in terms of the field strength tensor by $E_j = F_{0j} = -iF_{0j}^{(M)} = iE_j^{(M)}$ and $B_j = -\frac{1}{2}\varepsilon_{lmj}F_{lm} = -\frac{1}{2}\varepsilon_{lmj}F_{lm}^{(M)} = B_j^{(M)}$, where ε_{ijk} is the fully antisymmetric Levi-Civita tensor and the field strength tensor is given on the lattice by Eq. 26.

The heavy quark propagator is diagonal in both spin and color, and is given in momentum space by

$$\begin{aligned}\tilde{G}_Q(k) &= \left(1 - e^{-ik_0} F^{2n}(k)\right)^{-1}, \\ F(k) &= 1 - \frac{1}{nM} \sum_{j=1}^3 \sin^2(\frac{1}{2}k_j).\end{aligned}$$

The light quark propagator is diagonal in color:

$$\tilde{G}_q(k) = \left(i \sum_\mu \gamma_\mu \sin k_\mu + 2r \sum_\mu \sin^2(\frac{1}{2}k_\mu) + m\right)^{-1}.$$

In this paper, we work only with the $m = 0$ and $r = 1$ case. The gluon propagator is diagonal both in color and the Lorentz indices, and is given in Feynman gauge by

$$\tilde{G}_G(k) = \left(4 \sum_\mu \sin^2(\frac{1}{2}k_\mu) + \lambda^2\right)^{-1}.$$

We now list the vertex factors associated with the interaction of a single gluon with a heavy-quark line. Let k' be the outgoing heavy-quark momentum, k be the incoming quark momentum, and μ be the polarization index of the emitted gluon. These vertex factor all have a color factor of T_{bc}^a , where a is the color index of the gluon, and b and c are the color indices of the outgoing and incoming quarks, respectively. For $\mu = 0$, the vertex factor is

$$-ige^{-i(k'+k)_0/2} F^n(k) F^n(k').$$

For $\mu = j = 1, 2, 3$, the vertex factor from the $\mathbf{p}^2/2M$ term is

$$-g \frac{1}{2nM} \sin[\frac{1}{2}(k' + k)_j] \left[e^{-ik'_0} F^n(k') + e^{-ik_0} F^n(k) \right] S_n(k', k),$$

$$S_n(k', k) = \sum_{l=0}^{n-1} F^l(k') F^{n-l-1}(k).$$

For $\mu = j$ from the $\boldsymbol{\sigma} \cdot \mathbf{B}$ term, the vertex factor is given by

$$g \sum_{r,s} \frac{1}{4M} (\gamma_5 \gamma_0 \gamma_r) \epsilon_{rsj} \sin(k' - k)_s \cos[\frac{1}{2}(k' - k)_j] \left[e^{-ik'_0} F^{2n}(k') + e^{-ik_0} F^{2n}(k) \right].$$

The single-gluon vertex factor for the light quark (clover action) is

$$-g \left\{ i\gamma_\mu \cos[\frac{1}{2}(k' + k)_\mu] + r \sin[\frac{1}{2}(k' + k)_\mu] + \frac{r}{2} \sum_\nu \sigma_{\nu\mu} \sin(k' - k)_\nu \cos[\frac{1}{2}(k' - k)_\mu] \right\},$$

for all gluon polarizations μ , where k' (k) is the outgoing (incoming) momentum of the light quark.

Next, the vertex factors associated with the interaction of two gluons with a heavy-quark line are given. Let k' be the outgoing heavy-quark momentum, k be the incoming quark momentum, and q_1, q_2 be the outgoing momenta of the emitted gluons having polarization indices μ_1, μ_2 , respectively. Only the factors for $\mu_1 = \mu_2$ (and $q_1 + q_2 = 0$) are given, which is all that is required for the one-loop tadpole graphs. The color factor for these cases is $(T^a T^{a'})_{bc}$, where a, a' are the color indices of the gluons, and b and c are the color indices of the outgoing and incoming quarks, respectively. For $\mu_1 = \mu_2 = 0$, the vertex factor is

$$-\frac{g^2}{2} e^{-i(k'+k)_0/2} F^n(k') F^n(k).$$

For $\mu_1 = \mu_2 = j$, the vertex factor from the $\mathbf{p}^2/2M$ term in the NRQCD action is

$$g^2 \left[e^{-ik'_0} F^n(k') + e^{-ik_0} F^n(k) \right] \left(\frac{-1}{4nM} \cos[\frac{1}{2}(k'+k)_j] S_n(k', k) \right.$$

$$+ \frac{1}{(2nM)^2} \sin[\frac{1}{2}(k'+k-q_2)_j] \sin[\frac{1}{2}(k'+k+q_1)_j] S_{g,n}(k', k' + q_1, k) \Big)$$

$$+ g^2 \frac{1}{(2nM)^2} \sin[\frac{1}{2}(k'+k-q_2)_j] \sin[\frac{1}{2}(k'+k+q_1)_j] S_n(k', k - q_2) S_n(k' + q_1, k) e^{-i(k'+q_1)_0},$$

where

$$S_{g,n}(k', k' + q_1, k) = \sum_{l \geq 0}^{n-2} F^l(k') S_{n-l-1}(k' + q_1, k).$$

The vertex factor for $\mu_1 = \mu_2 = j$ from the $\boldsymbol{\sigma} \cdot \mathbf{B}$ term is

$$g^2 \frac{1}{(4M)^2} \sum_{r,s,r',s'} e^{-i(k'+q_1)_0} F^{2n}(k' + q_1) (\gamma_5 \gamma_0 \gamma_r) (\gamma_5 \gamma_0 \gamma_{r'}) \epsilon_{rsj} \epsilon_{r's'j}$$

$$\times \sin(k' - k + q_2)_s \sin(k' - k + q_1)_{s'} \cos[\frac{1}{2}(k' - k + q_2)_j] \cos[\frac{1}{2}(k' - k + q_1)_j]$$

$$+ \text{terms that vanish for } q_1 + q_2 = 0.$$

The heavy-light currents, $J_{A,\text{lat}}^{(i)}$, are not part of the action and we list their Feynman rules separately. Again, let k' and k be the outgoing and incoming quark momenta, respectively, and let q_i and μ_i denote the momenta and polarizations, respectively, of the emitted gluons. Also, let q_{ext} be the momentum carried off by external heavy-light current, where $k = k' + \sum_i q_i + q_{\text{ext}}$. We use the notation $[O]^{(n)}$ to indicate the vertex factor for n -gluon emission from operator O . At tree level,

$$\begin{aligned} \left[J_{A,\text{lat}}^{(1)} \right]^{(0)} &= -\frac{i}{2M} \sum_j \sin[\tfrac{1}{2}(k' + k + q_{\text{ext}})_j] (\Gamma \gamma_j), \\ \left[J_{A,\text{lat}}^{(2)} \right]^{(0)} &= -\frac{i}{2M} \sum_j \sin[\tfrac{1}{2}(k' + k - q_{\text{ext}})_j] (\gamma_j \Gamma). \end{aligned}$$

For one gluon emission ($\mu = j$, color factor = T_{bc}^a):

$$\begin{aligned} \left[J_{A,\text{lat}}^{(1)} \right]^{(1)} &= -g \frac{i}{2M} \cos[\tfrac{1}{2}(k' + k + q_{\text{ext}})_j] (\Gamma \gamma_j), \\ \left[J_{A,\text{lat}}^{(2)} \right]^{(1)} &= -g \frac{i}{2M} \cos[\tfrac{1}{2}(k' + k - q_{\text{ext}})_j] (\gamma_j \Gamma). \end{aligned}$$

For two gluon emission ($\mu_1 = \mu_2 = j$, color factor = $(T^a T^{a'})_{bc}$):

$$\begin{aligned} \left[J_{A,\text{lat}}^{(1)} \right]^{(2)} &= g^2 \frac{i}{4M} \sin[\tfrac{1}{2}(k' + k + q_{\text{ext}})_j] (\Gamma \gamma_j), \\ \left[J_{A,\text{lat}}^{(2)} \right]^{(2)} &= g^2 \frac{i}{4M} \sin[\tfrac{1}{2}(k' + k - q_{\text{ext}})_j] (\gamma_j \Gamma). \end{aligned}$$

REFERENCES

- [1] E. Eichten, Nucl. Phys. B (Proc. Suppl.) **4**, 170 (1988).
- [2] B.A. Thacker and G.P. Lepage, Phys. Rev. D**43** 196 (1991).
- [3] G.P. Lepage *et al.*, Phys. Rev. D**46** 4052, (1992).
- [4] A.X. El-Khadra, A.S. Kronfeld, P.B. Mackenzie, Phys. Rev. D**55**, 3933 (1997).
- [5] A. Ali Khan *et al.*, Phys. Rev. D **56**, 7012 (1997).
- [6] A. Ali Khan *et al.*, in preparation.
- [7] B. Sheikholeslami and R. Wohlert, Nucl. Phys. B**259**, 572 (1985).
- [8] O. Hernandez and B. Hill, Phys. Rev. D**50**, 495 (1994).
- [9] P. Bouchard, C. Lin, and O. Pene, Phys. Rev. D**40**, 1529 (1989); D**41**, 3541(E) (1990).
- [10] P. Boucaud *et al.*, Phys. Rev. D**47**, 1206 (1993).
- [11] M. Golden and B. Hill, Phys. Lett. B**254**, 225 (1991).
- [12] L.L. Foldy and S.A. Wouthuysen, Phys. Rev. **78**, 29 (1950).
- [13] G.P. Lepage and P.B. Mackenzie, Phys. Rev. D**48**, 2250 (1993).
- [14] See, for example, C. Bendtsen and O. Stauning, Technical Report IMM-REP-1997-07, Dept. of Mathematical Modelling, Technical University of Denmark, 1997 (unpublished), and references contained therein.
- [15] G.P. Lepage, J. Comput. Phys. **27**, 192 (1978).
- [16] K. Jansen *et al.*, Phys. Lett. B**372**, 275 (1996).
- [17] C. Morningstar, Phys. Rev. D**50**, 5902 (1994).
- [18] G. Martinelli and C. Sachrajda, Nucl. Phys. B**478**, 660 (1996).
- [19] C. Morningstar, Phys. Rev. D**48**, 2265 (1993).

FIGURES

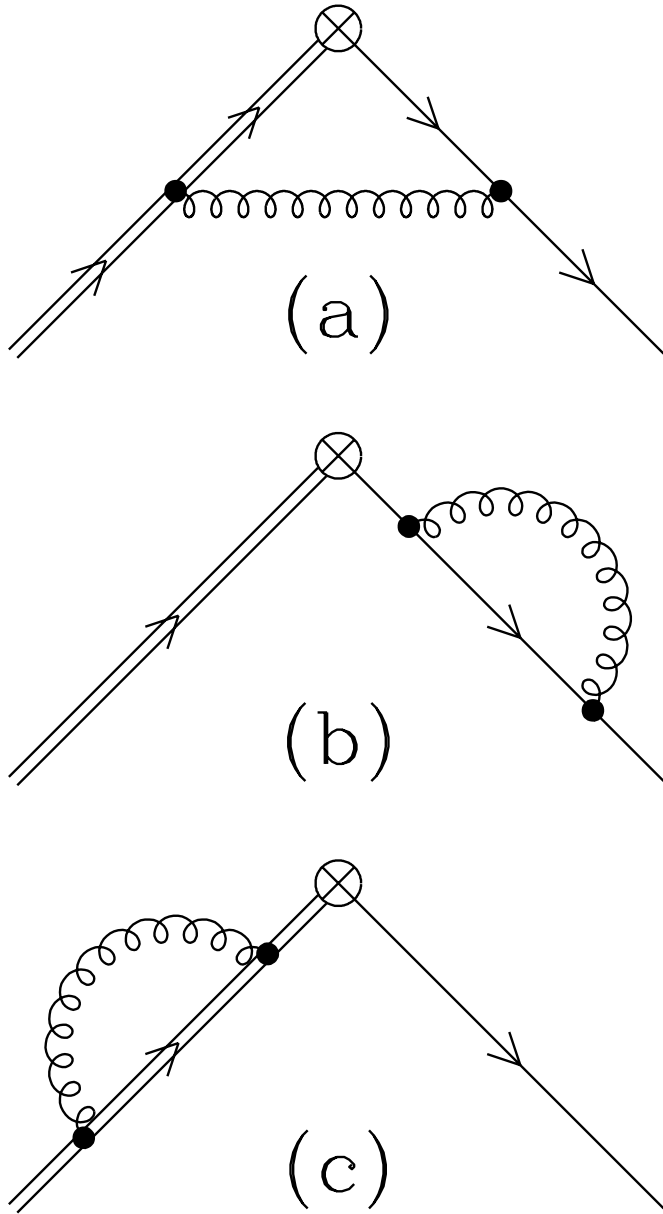


FIG. 1. Feynman diagrams in continuum and lattice perturbation theory which contribute at one-loop order to the annihilation by the axial current (cross inside a circle) of an incoming heavy quark (double solid line) and the creation of an outgoing light quark (single solid line). The exchange of a gluon is denoted by a curly line.

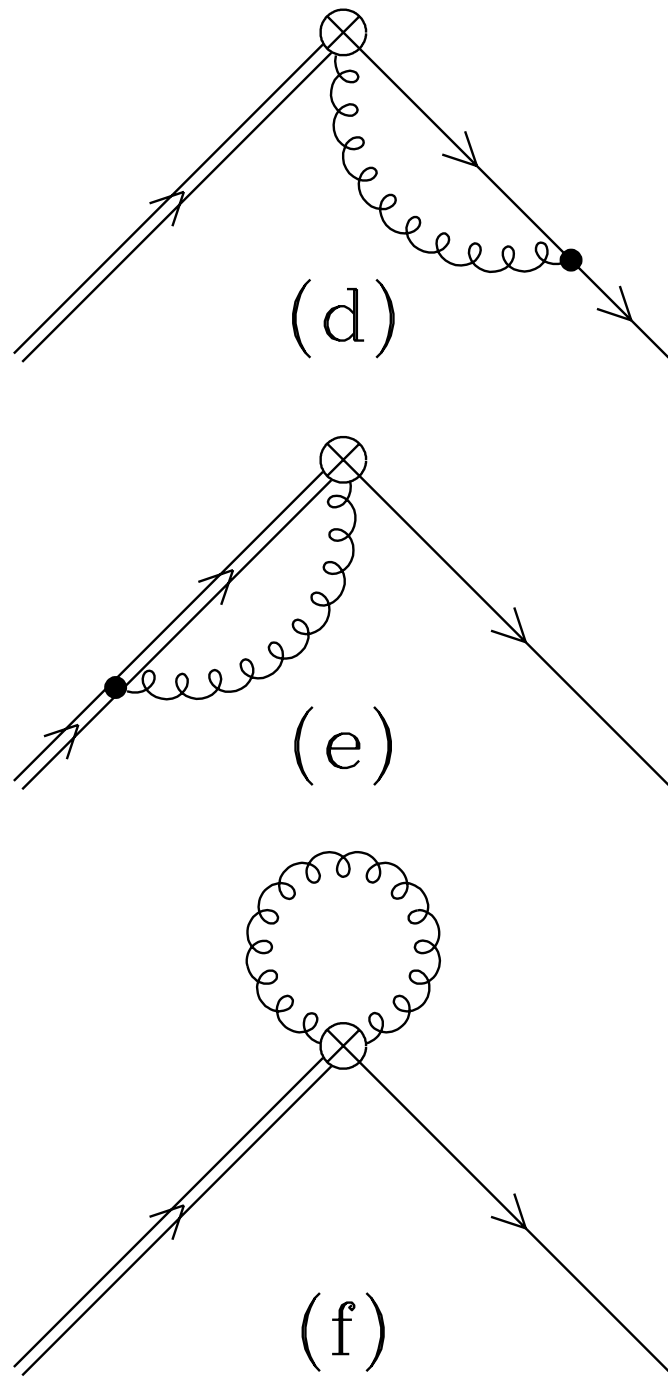


FIG. 2. Additional vertex correction diagrams which contribute in *lattice* perturbation theory to the same process as in Fig. 1.

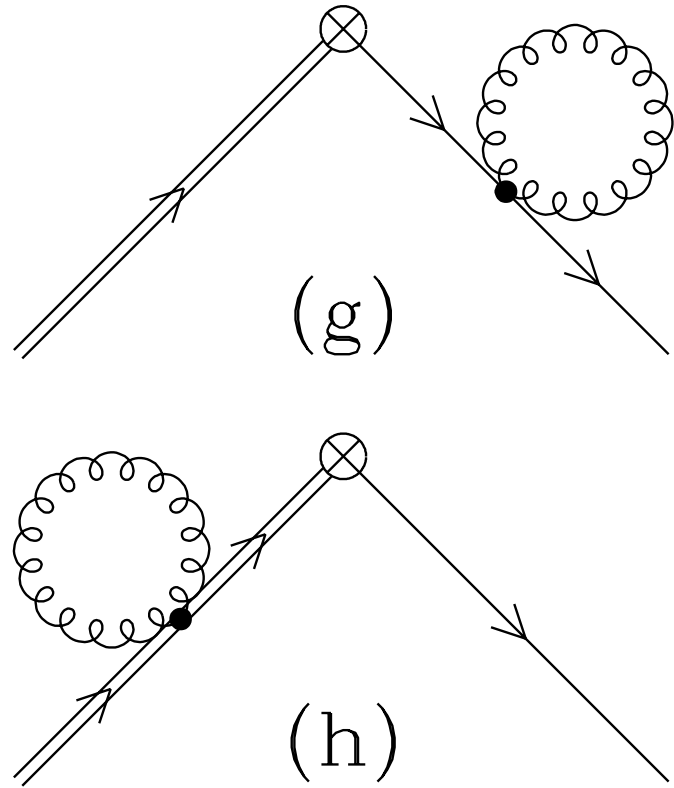


FIG. 3. Additional external leg correction diagrams which contribute in *lattice* perturbation theory to the same process as in Fig. 1.

TABLES

TABLE I. Values of the coefficients τ_0 , τ_1 , τ_2 , C_Q , and C_m appearing in Eq. 33 for various values of the bare heavy-quark mass aM_0 and NRQCD stability parameter n . Uncertainties in the determinations of these parameters due to the use of Monte Carlo integration are included.

aM_0	n	τ_0	τ_1	τ_2	C_Q	C_m
10.0	1	0.8232(1)	-1.242(4)	-14.74(2)	0.2719(8)	0.872(8)
7.0	1	0.7929(1)	-1.266(1)	-8.82(2)	0.1847(6)	0.862(6)
4.0	1	0.7290(1)	-1.283(2)	-3.202(8)	-0.0287(6)	0.883(6)
4.0	2	0.7397(1)	-1.298(2)	-3.476(8)	-0.0030(6)	1.087(6)
3.5	2	0.7239(1)	-1.307(2)	-2.618(8)	-0.0651(6)	1.120(6)
3.0	2	0.7052(1)	-1.315(2)	-1.790(8)	-0.1463(6)	1.142(6)
2.7	2	0.6923(1)	-1.324(2)	-1.314(4)	-0.2077(6)	1.172(6)
2.5	2	0.6829(1)	-1.332(2)	-1.010(4)	-0.2562(6)	1.195(6)
2.0	2	0.6576(1)	-1.352(1)	-0.304(3)	-0.4156(6)	1.235(4)
1.7	2	0.6422(1)	-1.371(2)	0.081(3)	-0.5503(8)	1.277(4)
1.6	2	0.6377(1)	-1.377(1)	0.202(3)	-0.6038(8)	1.293(6)
1.2	3	0.6307(1)	-1.424(1)	0.538(2)	-0.868(1)	1.557(6)
1.0	4	0.6365(1)	-1.457(1)	0.683(2)	-1.074(1)	1.733(6)
0.8	5	0.6617(1)	-1.502(1)	0.818(1)	-1.394(1)	1.934(6)

TABLE II. Values for the coefficients ρ_0 , ρ_1 , and ρ_2 appearing in Eq. 38.

aM_0	n	ρ_0	ρ_1	ρ_2
10.0	1	-0.2972(4)	0.315(9)	-3.982(24)
7.0	1	-0.3368(3)	0.212(6)	-3.902(16)
4.0	1	-0.3443(3)	-0.032(6)	-3.525(8)
4.0	2	-0.3679(3)	-0.038(6)	-3.251(8)
3.5	2	-0.3635(3)	-0.102(6)	-3.109(8)
3.0	2	-0.3533(3)	-0.161(6)	-2.937(8)
2.7	2	-0.3433(3)	-0.214(6)	-2.813(4)
2.5	2	-0.3341(3)	-0.253(6)	-2.717(4)
2.0	2	-0.3002(3)	-0.343(4)	-2.423(3)
1.7	2	-0.2691(4)	-0.420(4)	-2.208(3)
1.6	2	-0.2571(4)	-0.451(6)	-2.128(3)
1.2	3	-0.2096(6)	-0.572(6)	-1.664(2)
1.0	4	-0.1703(7)	-0.627(6)	-1.410(2)
0.8	5	-0.1069(7)	-0.694(6)	-1.144(1)

TABLE III. Values for the coefficients ρ_0 , ρ_1 , and ρ_2 using the NRQCD action of Ref. [6].

aM_0	n	ρ_0	ρ_1	ρ_2
10.0	1	-0.2772(4)	0.45(1)	-4.70(3)
7.0	1	-0.3174(4)	0.322(7)	-4.38(2)
4.0	1	-0.3372(3)	0.140(7)	-3.643(8)
2.7	2	-0.3375(4)	0.027(4)	-2.859(4)
2.0	2	-0.3145(4)	-0.037(4)	-2.339(4)
1.6	2	-0.2844(4)	-0.054(4)	-1.986(3)